Title	DETECTION OF CORROSION-INDUCED DAMAGE IN REINFORCED CONCRETE BEAMS BASED ON STRUCTURAL DAMPING IDENTIFICATION
Author(s)	SHAHZAD, S.; YAMAGUCHI, H.; TAKANAMI, R.; ASAMOTO, S.
Citation	Proceedings of the Thirteenth East Asia-Pacific Conference on Structural Engineering and Construction (EASEC-13), September 11-13, 2013, Sapporo, Japan, G-2-4., G-2-4
Issue Date	2013-09-13
Doc URL	http://hdl.handle.net/2115/54415
Type	proceedings
Note	The Thirteenth East Asia-Pacific Conference on Structural Engineering and Construction (EASEC-13), September 11-13, 2013, Sapporo, Japan.
File Information	easec13-G-2-4.pdf

DETECTION OF CORROSION-INDUCED DAMAGE IN REINFORCED CONCRETE BEAMS BASED ON STRUCTURAL DAMPING IDENTIFICATION

S. SHAHZAD[1†], H. YAMAGUCHI[2*], R. TAKANAMI[2] and S. ASAMOTO[2]

[1]*National Engineering Services, Pakistan Pvt. Ltd. Lahore, Pakistan (formerly, Saitama Univ.)*
[2]*Graduate School of Science and Engineering, Saitama University, Japan*

ABSTRACT

This article examines the possibility of corrosion damage detection in reinforced concrete (here after RC) beams based on modal damping changes. Four RC beams were damaged artificially by inducing uniform and localized corrosions on the beams. Modal tests were performed on the test beams before and after the corrosion damages, and extracted modal parameters were compared with each other. The result showed certain amount of changes in modal parameters, namely natural frequency and modal damping ratio, and the modal damping ratio was more sensitive than the natural frequency against corrosion-induced damages. This indicates that the local and small corrosion damage might be detectable by monitoring the modal damping ratio of RC structures.

Keywords: Reinforced concrete beam, corrosion damage, dynamic testing, modal damping, natural frequency.

1. INTRODUCTION

Deterioration of existing concrete structures is a serious problem all over the world. The deterioration of RC structures may be results of insufficient reinforcement, large deflection, poor concrete quality and steel corrosion linked to environmental conditions. Past investigation and survey (Capozucca 2008;Wallbank 1989) have revealed that major form of deterioration in RC structures is reinforcement corrosion. Due to the reinforcement corrosion, there is a loss of bond between the steel bar and the concrete as well as micro cracking inside the concrete. These factors have relevant influence on the load carrying capacity of RC members. Because the corrosion occurs inside concrete structures and invisible, this invisible damage might not be detected by field static testing and/or traditional visual inspection method. Therefore, it is an urgent need to detect these damages at their earliest stages so that some remedial action can be taken to minimize or prevent the catastrophic failures, which may lead to injuries, fatalities and loss of property. To assist in assessing the structural integrity of RC structures against small and local corrosion damages, the structural health monitoring based on vibration characteristics changes might be useful.

---

[*] Corresponding author: Email: hiroki@mail.saitama-u.ac.jp

[†] Presenter: Email:engr.shahzadsaeed@gmail.com

This paper reports on the corrosion-induced damages in RC beams, which are experimentally investigated through dynamic modal testing. The aim of this study is to detect the corrosion damage in RC beams by the identification of modal damping changes.

2. TEST SPECIMEN AND ACCELERATED CORROSION TEST

Four RC beams were casted in the laboratory. The size of beam was 600 mm in length, 70 mm in height and 100 mm in width. The beams were corroded by artificial impressed current technique (Rinaldi et al. 2010) in which the test beam was immersed in 5% Nacl solution and electric current impressed on the steel. The positive terminal of battery connected to the tensile reinforcement of test beam and the negative terminal connected to the stainless steel bar. Two different corrosion-patterns, namely uniform corrosion (denoted as *U*) and localized corrosion (denoted as *L*), were induced on the beams. In the uniform corrosion, the beam reinforcement was corroded throughout the length, while the central 100 mm portion of beam reinforcement was corroded in the localized corrosion. The experimental setup used for these corrosion patterns is illustrated in Figure 1.

In the localized corrosion, a stainless steel plate with two sponges was used and the saline solution was given to the local area of test beam through the sponge, as shown in Figure 1(b). Before the corrosion process, the beam was kept in the saline solution for 24 hours in order to allow the saline solution to permeate inside the concrete cover and to reach the reinforcement.

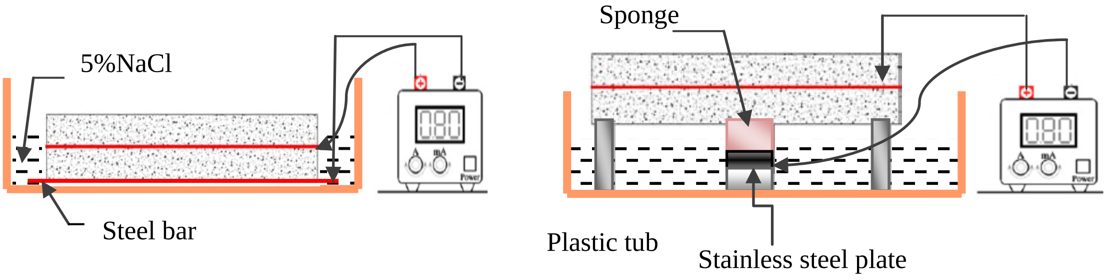

(a)

(b)

Figure 1:Experimental setups for (a) uniform corrosion and (b) localized corrosion.

The duration of corrosion process for achieving the selected corrosion level was set according to the Faraday's law, the expression of which is given in the following equation.

$$t = \alpha \frac{m_{loss} \cdot n_{specimen} \cdot C_{Far}}{I_{corr} \cdot M_{specimen}} \tag{1}$$

where α is a scale factor to account for the time lag of corrosion process caused by the protection of concrete cover, $M_{specimen}$ is the molar mass of reinforcement, $n_{specimen}$ is its valence, C_{Far} is the Faraday's constant (96500 Cmol^{-1}), I_{corr} is the imposed current in ampere, and t is the duration time in second. The corrosion amount and conditions are listed in Table1, and the extents as well as severity of damages in the uniformly and locally corroded beams are shown in Figure 2.

Table1: Corrosion amount and condition of beams

Uniform corrosion			Localized corrosion		
Beam	Corrosion (% mass loss)	Specimen condition	Beam	Corrosion (% mass loss)	Specimen condition
U_0	0	Undamaged	L_0	0	Undamaged
U_1	1.03	No visible crack	L_1	5.14	Minor cracks occurred along height and width directions
U_2	6.18	Visible cracks along the length	L_2	14.52	Major cracks occurred along height and width directions

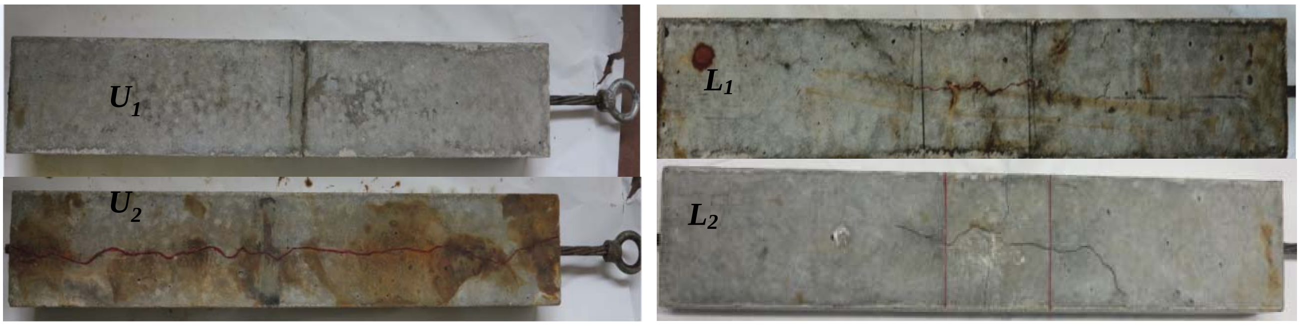

(a) (b)

Figure 2: Cracking pattern in (a) uniform corrosion and (b) local corrosion.

3. DYNAMIC TESTING AND DATA ANALYSIS

The schematic diagram of dynamic testing is illustrated in Figure 3. As shown in the figure, the beam was set in the free end condition in the dynamic testing, which was achieved by hanging the beam vertically with very thin wire at one end. The accelerometer was attached at the midpoint of beam to capture the 1st vertical bending mode. The beam was excited in the 1st vertical bending mode by giving the impact with an impact hammer at the midpoint of test beam on the opposite face of accelerometer attached.

For the repeatability purpose, the dynamic testing was performed five times on each test beam. The recorded duration of free vibration was 10 sec and the sampling frequency of 15000 Hz was used for avoiding the aliasing effect in the data analysis. After getting vibration data, the modal damping ratio was identified firstly by applying the conventional log-decrement method on the free vibration decay characteristics of beam. The log- decrement method is described in Eq. (2).

$$\delta = \frac{1}{n} ln \left[\frac{A_1}{A_n}\right] \tag{2}$$

where δ is the log-decrement value, A_1 is the initial amplitude value and A_n is the amplitude value after n cycles of vibration. From the log-decrement value in Eq. (2), the modal damping ratio is calculated as $\xi = \delta/2\pi$.

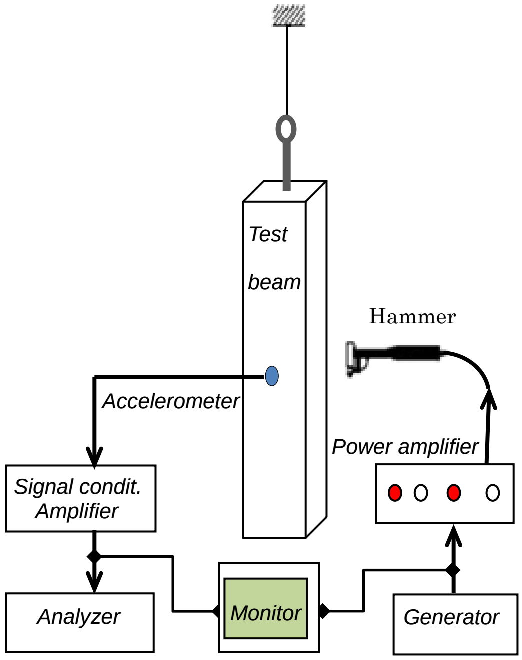

Figure 3:Schematic diagram of dynamic testing.

Secondly, the modal damping parameters are identified by applying the curve fitting method, with damping model proposed by Franchetti *et-al*. (2009), to the free decay vibration envelope. This model contain two damping parameters, namely the viscous damping ratio and the quadratic damping factor that represents the nonlinear damping as represented in Eq. (3).

$$a(t) = \frac{(a_0 c_1).e^{-c_1 t}}{c_1 + a_0 c_2 (1 - e^{-c_1 t})}, \qquad C_1 = \xi\omega, \qquad C_2 = \frac{4}{3\pi}\delta'\omega \tag{3}$$

whereω, ξ,δ',$a_0$and t are circular frequency, viscous damping ratio, quadratic damping factor, initial amplitude and time of one vibration cycle respectively.

4. RESULTS AND DISSCUSSIONS

4.1 Uniformly corroded beams

The modal damping ratios for the corroded and uncorroded beams identified by the log-decrement method are plotted in Figure 4(a), which shows the realtionship between the modal damping ratio and the vibration amplitude. The modal damping ratio is almost constant with the amplitude for each damage level. This indicates that the viscous damping governs the energy dissipation in this case.

Figure 4(b) shows the modal damping ratio indentified by the curve fitting method with the nonlinear damping model. The modal damping ratios identified by the curve fitting method are nearly equal to the averaged values identified by the log-decrement method for all the damge levels.

The modal damping ratio represents the energy dissipation within the system. In the undamaged system, the energy induced by the excitation force is imparted to the system and solely utilized for the vibratory motion of system. In the case that the damage is present in the system, however, some of the excitation energy is entrapped and dissipated through the defects, thus leaving less energy for the vibratory motion. This trend of energy dissipation is observed in the corroded and healthy beams in Figure 4, where the modal damping ratio is increased with the increase of the corrosion damage level. It is noted that the damping model is dominated by the viscous damping without any contribution of nonlinear damping in the uniformly corroded case, as shown in Figure 5(a) where the comparison is made in the exponentially decaying envelope between experimentally obtained one and identified one by using Eq. (3). In the case of uniform corrosion, the crack occured in the direction of steel rainforcementas shown in Figure 2(a), and this type of cracking does not affect significantly on the transverse dynamics of beam. Therefore, the changes in the modal damping ratio could be related mainly to the microfracturing in the concrete volume rather than the cracking.

The changing trend of modal damping ratio is more sensitive than that of natural frequency to the corrosion damage in RC beams, as shown in Figure 5(b). The changes in the natural frequency of corroded beams as compared to the undamaged beam are very small, that is, 0.67% and 2.6 % for the

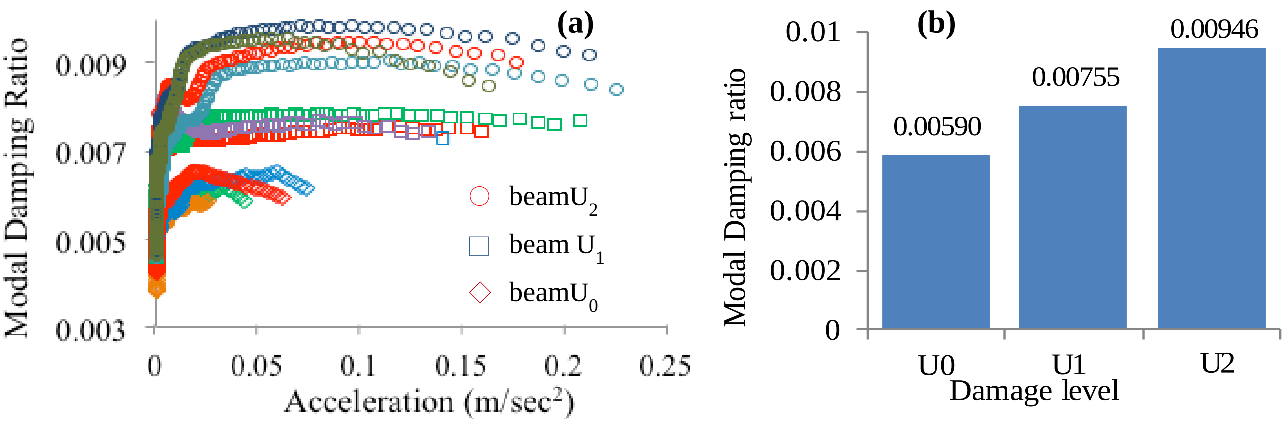

Figure 4: Modal damping ratio of uniformly corroded and un-corroded beams identified by (a) log-decrement method and (b) curve fitting method.

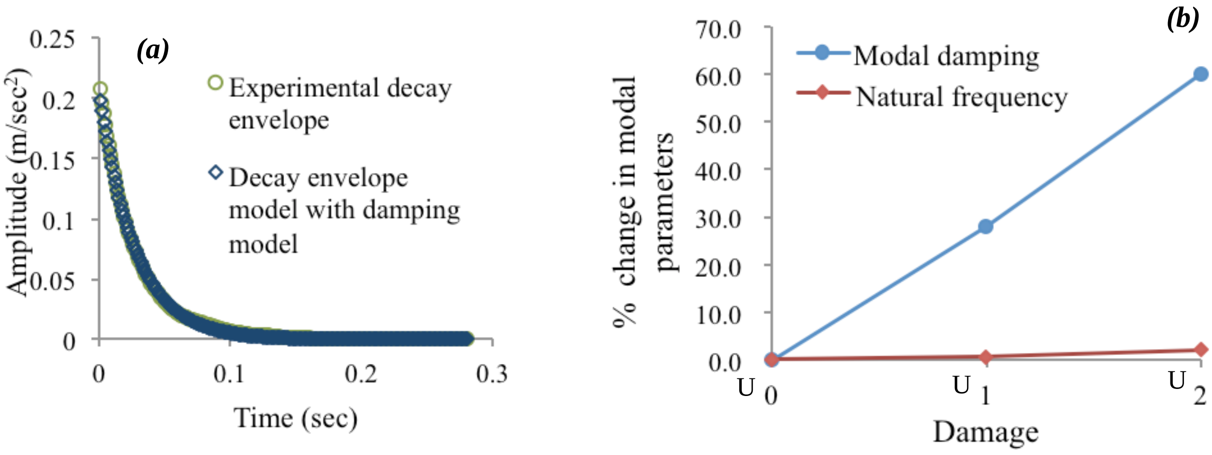

Figure 5: (a) Curve fitting with damping model to vibration decay envelope and (b) changes in modal parameters with different corrosion damages.

corroded beams U_1 and U_2, respectively. On the other hand, the changes in the modal damping ratio are relatively large, that is, 28% and 59% for the corroded beams $U_1$and U_2, respectively.

4.2 Locally corroded beams

In the case of local corrosion, an unstable phenomenon was observed in the dynamic testing. That is, the charcteristics of free vibration response changes every time the impact testing is repeated, as shown in Figur 6. This unstable phenomenon might be due to unstable surface crack condition, which could be changed by every impact force. That is, initially in the corroded beam, there might exist some loose particles and corrosion products inside the cracks and the crack surface condition could be stablized after the loose particles and corrosion products are forced to be removed from the cracks by th ehammering impact. This observation is understood from Figure 6, where the frictional damping becomes more and more dominant and the response frequency becomes smaller and smaller every time the hummering impact is repeatedly applied. The unstable crack surface condition has an effect on both the response frequency and the modal damping characteristics.

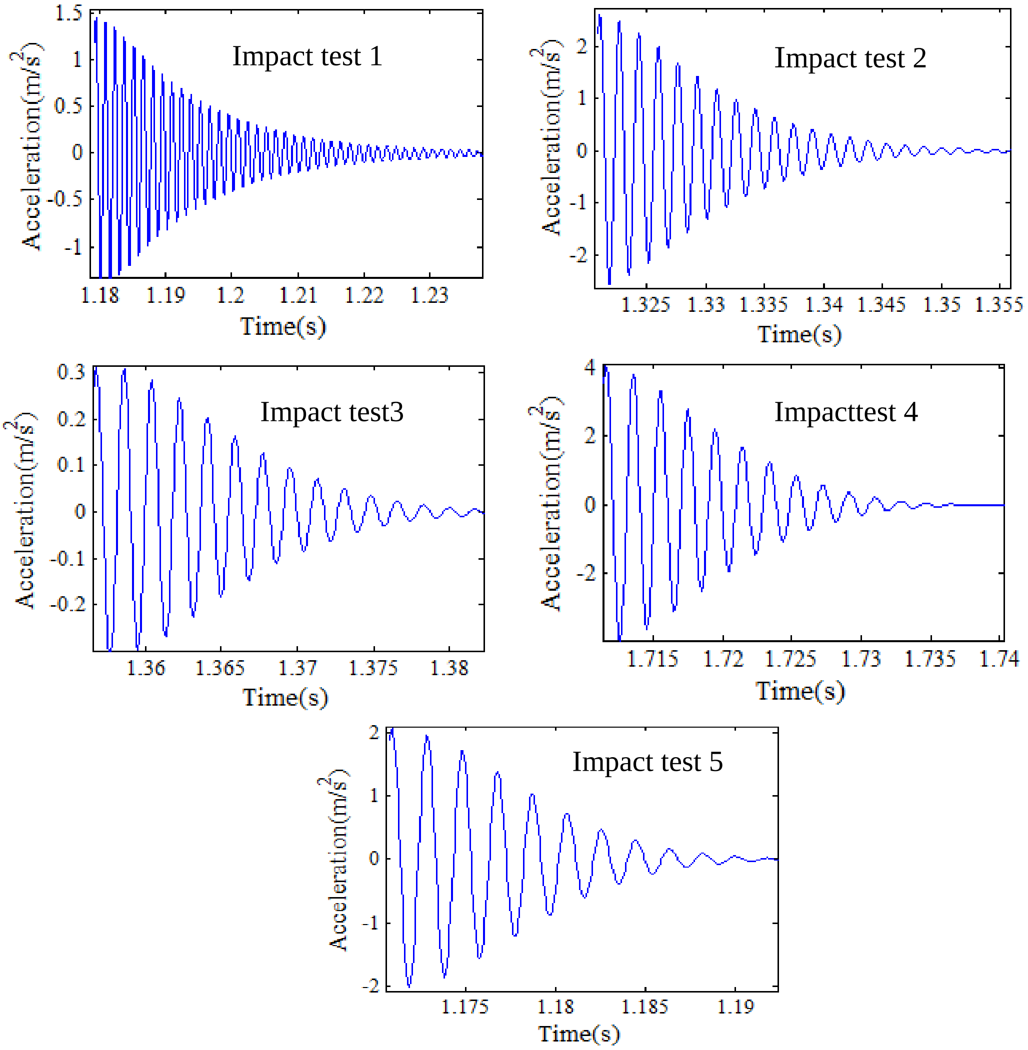

Figure 6: Free decay vibration characteristics of locally corroded beam L_1 for repeating the impact testing five times.

Figure 7 shows the changes of natural freuency and associated modal damping parameters in Eq. (3) with every impact test. The natural frequency converges to the stable value after the third impact test as shown in Figure 7(a), which means that the crack condition becomes stable at this stage. The modal damping parameters are also increased as a whole on every impact, as shown in Figure 7(b) where the viscous damping parameter as well as the nonlinear damping parametre corresponding to the friction damping identified by thecurve fitting method are indicated. It should be noted that, in the cases of locally corrded beams, the damping characteristics are governedalmost equally by the viscous and nonlinear damping. This damping charcteristics of locally corroded beams can be explained by the fact that the cracks are induced in both the longitudnal and tranverse directions as shown in Figure 2(b). That is, a certain amount of exciting energy can be dissipated through the frcition between the crack surfaces as well as that in the steel-concrete interface, and a significant contribution of nonlinear damping appears in the total damping of locally corroded specimen. It is also seen in Figure 7(b) that the nonlinear damping is increased upto the fourth testing and then decreased. This might be caused by

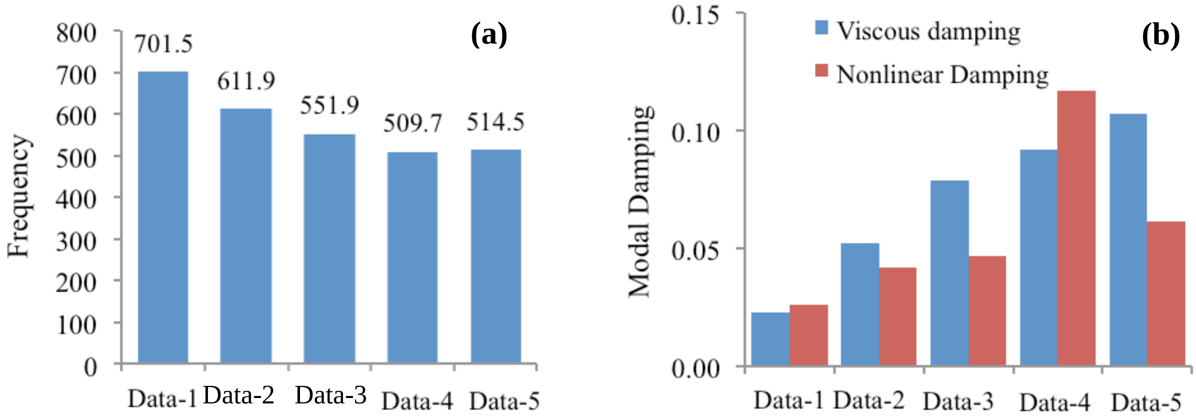

Figure 7: Results of locally corroded beam L_1: (a) frequency drop and (b) increase of viscous and nonlinear damping induced by 5 times repeated impact testing.

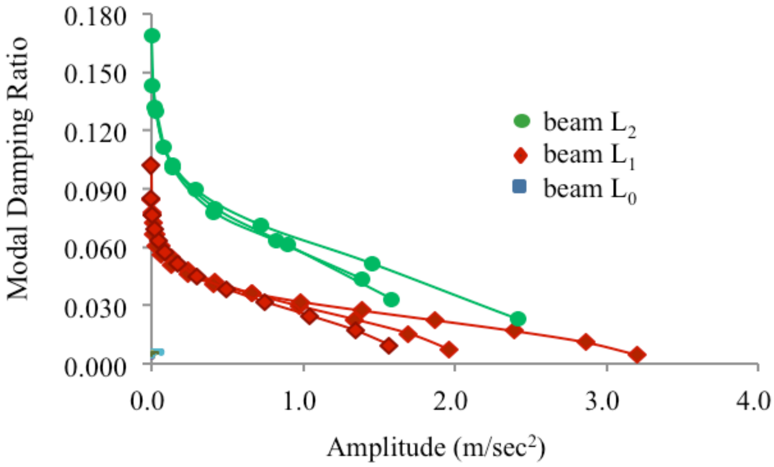

Figure 8: Modal damping ratios of locally corroded and un-corroded beams identified by log-decrement method.

the cracks fully opened at the fifth stage offering less friction between the crack surfaces. It is also understood from Figure 7 that siginificant changes occur in the natuaral frequency in the localized corrosion damage but that the modal damping is more sensitive than the frequency to the damage level.

The modal damping ratio was identified by the log-decrement method even for the locally corroded beams after the free vibration was stabilized at the fifth hammering. Figure 8 shows thus identified modal damping ratios for two corrosion levels L_1 and L_2. The modal damping ratios of different corrosion levels are well separated with each other, while the strong amplitude dependence of modal damping ratio exists, indicating that the local corrosion might be detectable by measuring the modal damping ratio of RC structures.

5. CONCLUSIONS

The modal damping ratio is a very sensitive indictor against the corrosion-induced damages in the RC beams. Detectable changes can occur in the modal damping ratio against even small and local corrosion damages without visible cracks in the concrete beams. This indicates the possibility of detecting localized and small corrosion damages in concrete structures based on the identification of modal damping changes.

REFERENCES

Capozucca R. (2008), Detection of damage due to corrosion in prestressed RC beam by static and dynamic tests, Construction and Building Materials, **22**: 738–74.

Chen G.D, Yang, X.B and Mu, H.M (2000), Stability of nonlinear vibration in cracked concrete structures, Proc. International Conference on Advance Problems in Vibration Theory and Application, China: 457-462.

Ewins D. (2006), Modal testing, 2nd Edition, Research Studies Press Ltd. England.

Franchetti P., Modena C. and Feng, M.Q (2009), Nonlinear damping identification in precast prestressed reinforced concrete beams, Computer-Aided Civil and infrastructure Engineering,**24(8):** 577-592.

Rinaldi Z., Imperatore S. and Valente C. (2010), Experimental evaluation of the flexural behavior of corroded P/C beams, Construction and Building Materials, **24(11)**: 2267-2278.

Wallbank R.J (1989), The performance of concrete in bridges: a survey of 200 highway bridges, Department of Transportation, London.